Proceedings of the Combustion Institute, Volume 28, 2000/pp. 2021–2027

SIMULTANEOUS PARTICLE-IMAGING VELOCIMETRY AND OH PLANAR LASER-INDUCED FLUORESCENCE MEASUREMENTS IN AN UNSTEADY COUNTERFLOW PROPANE/AIR DIFFUSION FLAME

ERIC J. WELLE,[1] WILLIAM L. ROBERTS,[1] MICHELE E. DECROIX,[2] CAMPBELL D. CARTER[3] AND JEFFREY M. DONBAR[4]

[1]*North Carolina State University*
Department of Mechanical and Aerospace Engineering
Box 7910
Raleigh, NC 27695-7910, USA
[2]*Los Alamos National Laboratory*
Group DX-2, High Explosives Science and Technology
Los Alamos, New Mexico 87545, USA
[3]*Innovative Scientific Solutions, Inc.*
2786 Indian Ripple Road
Dayton, OH 45440-3638, USA
[4]*Air Force Research Laboratory, AFRL/PRSS*
Wright-Patterson Air Force Base, OH 45433-7103, USA

To study the transient response of a diffusion flame to an unsteady flowfield, quantitative measurements of velocity, using particle-imaging velocimetry, and OH measurements, using planar laser-induced fluorescence, were made simultaneously in an oscillating counterflow diffusion flame. These non-intrusive measurements were performed to spatially and temporally resolve flowfield and flame characteristics as a function of initial steady strain rate and forcing frequency. For the forcing frequencies considered in this study, the strain rate fluctuations were found to lag the velocity fluctuations, but the phase difference decreased with increasing forcing frequency. At lower forcing frequencies, the width of the OH field responded quasi-steadily, but as the forcing frequency increased, the OH field showed transient effects. The dilatation velocity, defined as the difference between the minimum velocity in the preheat zone and the maximum velocity in the reaction zone, was used as a flame temperature indicator. The dilatation velocity revealed that the phase difference between the velocity and the temperature increased with increasing forcing frequency, confirming the existence of a diffusion limited response. The results presented here help to illuminate the interconnecting relationships between the chemistry, fluid dynamics, and reactant transport times.

Introduction

Turbulent diffusion flames are of particular interest because of their presence in most practical combustion devices. Flamelet theory is a method that characterizes turbulent diffusion flames as a collection of strained, laminar, one-dimensional flamelets [1,2] which are solely dependent upon the mixture fraction and instantaneous scalar dissipation rate. The flamelets are assumed to respond quasi-steadily to the unsteady strain rates of the turbulent flowfield. Recent computational and experimental studies, however, have shown that conditions exist where this assumption is invalid [3–6]. If the turbulent Reynolds number is sufficiently large, there exists a range of eddy sizes where the characteristic turnover time of the smallest eddies is comparable to the diffusion time of the laminar flamelet [3]. The large-scale eddies establish the magnitude of the mean strain rate, while the fluctuations around this mean value are caused by the smaller eddies. These conditions can lead to a wide range of characteristic frequencies [4]. Thus, it is necessary to investigate the frequency response of flamelets in an attempt to extend the applicability of the flamelet theory.

The purpose of this investigation was to quantify the strain rate and relative OH concentration fluctuations in a propane/air flame subjected to velocity fluctuations. A counterflow diffusion burner was used because it has the same scalar structure as a flamelet in the mixing zone of a turbulent reacting flowfield [1]. Particle-imaging velocimetry (PIV) measurements were used to quantify the velocity, strain rate, and phase-angle relationships between measured parameters as a function of velocity oscillation frequency. Simultaneously, the OH field was measured using planar laser-induced fluorescence (PLIF). Reaction zone thickness as measured by the

Report Documentation Page

Form Approved
OMB No. 0704-0188

1. REPORT DATE	2. REPORT TYPE	3. DATES COVERED
04 AUG 2000	**N/A**	**-**

4. TITLE AND SUBTITLE	5a. CONTRACT NUMBER
Simultaneous Particle-Imaging Velocimetry and OHPlanar Laser-Induced Fluorescence Measurements in an Unsteady Counterflow Propane/Air Diffusion Flame	5b. GRANT NUMBER
	5c. PROGRAM ELEMENT NUMBER
6. AUTHOR(S)	5d. PROJECT NUMBER
	5e. TASK NUMBER
	5f. WORK UNIT NUMBER
7. PERFORMING ORGANIZATION NAME(S) AND ADDRESS(ES) **North Carolina State University Department of Mechanical and Aerospace Engineering Box 7910 Raleigh, NC 27695-7910, USA**	8. PERFORMING ORGANIZATION REPORT NUMBER
9. SPONSORING/MONITORING AGENCY NAME(S) AND ADDRESS(ES)	10. SPONSOR/MONITOR'S ACRONYM(S)
	11. SPONSOR/MONITOR'S REPORT NUMBER(S)

12. DISTRIBUTION/AVAILABILITY STATEMENT
Approved for public release, distribution unlimited

13. SUPPLEMENTARY NOTES
See also ADM001790, Proceedings of the Combustion Institute, Volume 28. Held in Edinburgh, Scotland on 30 July-4 August 2000.

14. ABSTRACT

15. SUBJECT TERMS

16. SECURITY CLASSIFICATION OF:			17. LIMITATION OF ABSTRACT	18. NUMBER OF PAGES	19a. NAME OF RESPONSIBLE PERSON
a. REPORT	b. ABSTRACT	c. THIS PAGE			
unclassified	**unclassified**	**unclassified**	**UU**	**7**	

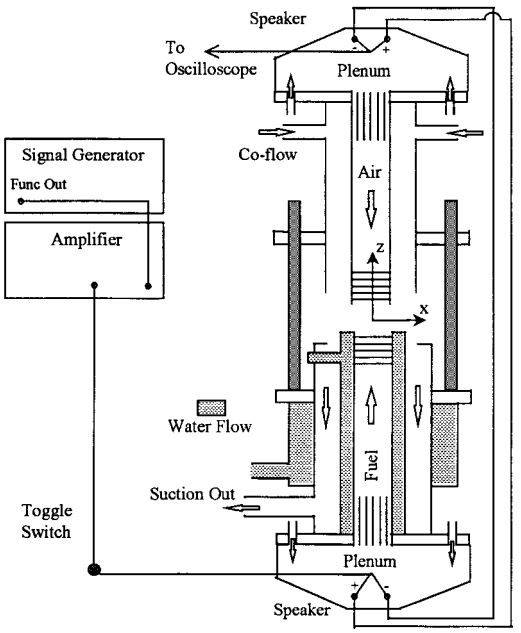

FIG. 1. Schematic of counterflow diffusion flame burner.

TABLE 1
Forcing Amplitude Shown as a Fraction of Flow Reversal and Extinction Voltages from Ref. [8]

	SSR 23 s^{-1}		SSR 44 s^{-1}		SSR 74 s^{-1}	
Freq. (Hz)	V V_{rev}	V V_{ext}	V V_{rev}	V V_{ext}	V V_{rev}	V V_{ext}
30	1	0.25	0.5	0.13	0.5	0.17
50	1	0.15	0.5	0.08	0.5	0.17
100	1	0.05	0.5	0.05	0.5	0.14
200	1	0.05	0.5	0.05	0.5	0.1

width of the OH field, rather than OH concentration, is presented in this paper.

Experimental Apparatus and Procedure

A schematic of the counterflow diffusion flame burner used in this study is shown in Fig. 1. The burner is a modification of the design described by Puri and Seshadri [7] and described in detail in Ref. [8]. Briefly, the oxidizer and fuel tubes are 25.4 mm in diameter and have a 12.7 mm separation distance. Plenums located on the fuel and oxidizer sides are capped with 20 cm loudspeakers, which impose the velocity fluctuations and are driven by an amplified signal generator.

An unsteady flowfield was imposed on the counterflow diffusion flame by inputting a sinusoidal voltage signal to the speakers. The velocity and relative [OH] measurements were made as a function of initial steady strain rate (SSR) and forcing frequency. These measurements were made at four temporal locations within the sinusoidal voltage oscillation applied to the speakers: the zero amplitude with positive slope (0+), maximum amplitude (Max), zero amplitude with negative slope (0−), and minimum amplitude (Min). The forcing frequencies considered in this study were 30, 50, 100, and 200 Hz. A weak forcing amplitude was applied to the flow; Table 1 defines this amplitude relative to flow reversal and extinction as previously measured [8].

Figure 2 is a schematic of the PIV-OH measurement system. The PIV measurements were made using two frequency-doubled Nd:YAG lasers (λ = 532 nm); in the probe region, the thickness of the two sheets were set to 500 μm with a height of 20 mm. Hollow zeospheres, having a mean diameter of 2.2 μm, were used to seed the airflow. The PIV images were recorded using a Kodak interline-transfer digital camera (1008 × 1012 pixels) fitted with a 105 mm lens, using an f stop of 8. An interference filter centered on 532 nm with a full width at half maximum (FWHM) of 3 nm was used to block background flame emission. Interrogation regions composed of 64 pixel squares (0.9 × 0.9 mm) with 75% overlapping were employed for the velocity measurements. Custom software including a cross-correlation algorithm was used to derive the velocities.

The OH measurements were made using a Nd:YAG pumped dye laser, which was running Rhodamine 590 dye, and the output of which was frequency doubled down to ~282 nm, yielding a 10 ns pulse of approximately 10 mJ in a sheet of approximately 300 μm in width and 20 mm in height. The $R_1(8)$ transition of the $A^2\Sigma^+ \leftarrow X^2\Pi(1,0)$ band was excited, partially saturating the transition, and detected using a Princeton Instruments Intensified Charge-Coupled Device (ICCD) camera. The $R_1(8)$ transition was chosen because of its reduced sensitivity to temperature fluctuations; indeed, the maximum OH concentration varied by less than 5% from the average cycle value for any of the experimental conditions. A 105 mm/f4.5 lens fitted with UG-11 and WG-295 filters was used to collect the OH fluorescence.

The response of the reaction zone to velocity oscillations was characterized by measuring the FWHM of the OH field. The strain rate was determined by evaluating the gradient of the axial velocity profile at the centerline of the burner on the oxidizer side of the stagnation plane. The centerline velocity was determined by averaging the three closest velocity vectors on both sides of the centerline that were at the same axial distance from the air tube exit.

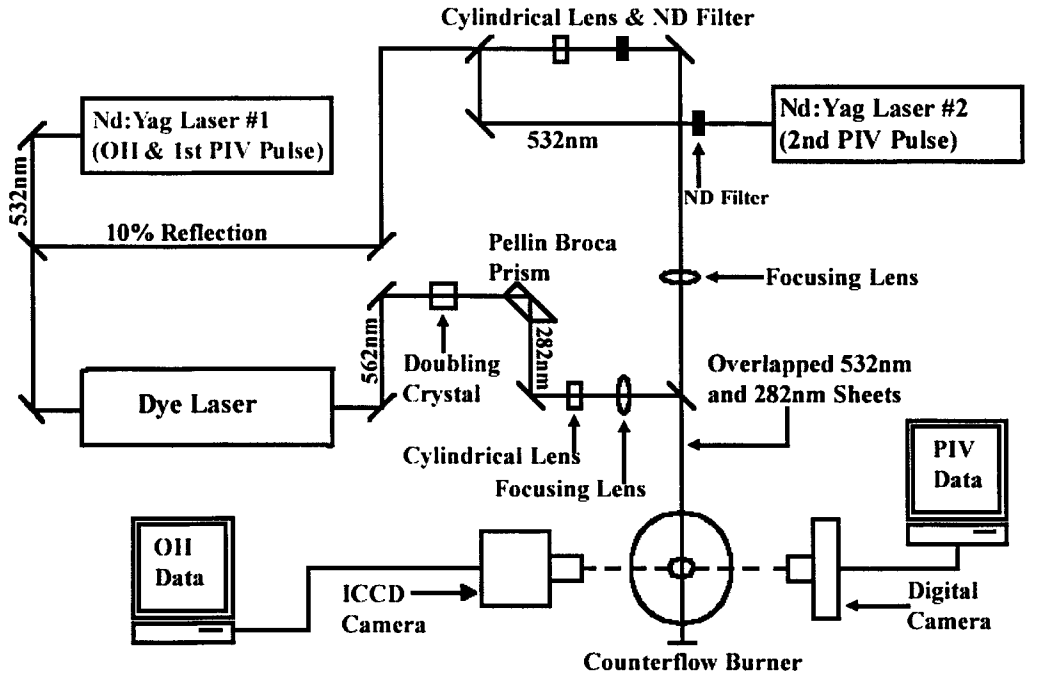

FIG. 2. Optical layout for PIV and OH-PLIF measurements.

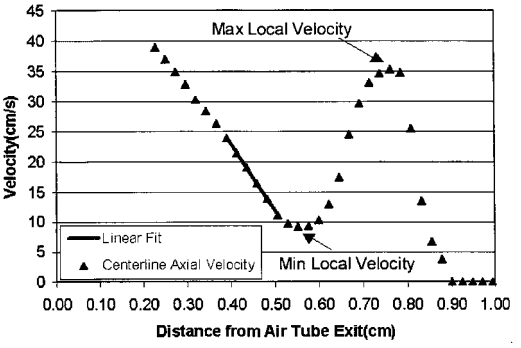

FIG. 3. Velocity field data showing the linear fitted line for strain rate calculations. Also shown are the velocities used to determine the dilatation velocity.

This averaged the velocity over 1.16 mm in the transverse coordinate at each axial position, which was less than 5% of the air tube exit diameter. A line was fit to the velocity data prior to the preheat zone, and the strain rate was then calculated from the fitted line. The location of the fitted line relative to the preheat zone is illustrated in Fig. 3. Twenty OH and PIV images were taken and averaged at each of the four temporal locations within the speaker oscillation. No corrections for thermophoretic effects have been performed on the velocity measurements, as previous studies have shown that accurate velocity measurements can be performed prior to the preheat zone without accounting for thermophoresis [9].

Results and Discussion

Due to the stoichiometry in a counterflowing propane/air diffusion flame, the flame is located on the air side of the stagnation plane. The transport of fuel is a result of diffusion, while the transport of oxidizer to the flame is a result of convection and diffusion. This convective-diffusive coupling on the air side effectively links the chemistry of the flame with the flowfield dynamics. A flame that is subject to a cyclical velocity field, with a characteristic cycle time much greater than that of any of the relevant transport times of the flame, should respond in a quasi-steady manner. As the characteristic cycle time of the velocity fluctuations decreases and approaches the relevant transport times of the flame, unsteady or transient characteristics in the flame behavior begin to appear.

The measured strain rates and FWHM of the OH field for an initial SSR of 74 s^{-1} are plotted in Fig. 4 at the four temporal locations in the speaker oscillation for all four forcing frequencies. At a forcing frequency of 30 Hz, the instantaneous strain rate continuously increases from the temporal locations of $0+$ to $0-$, as seen in Fig. 4a. During this period, the OH field narrows continuously. Between the $0-$

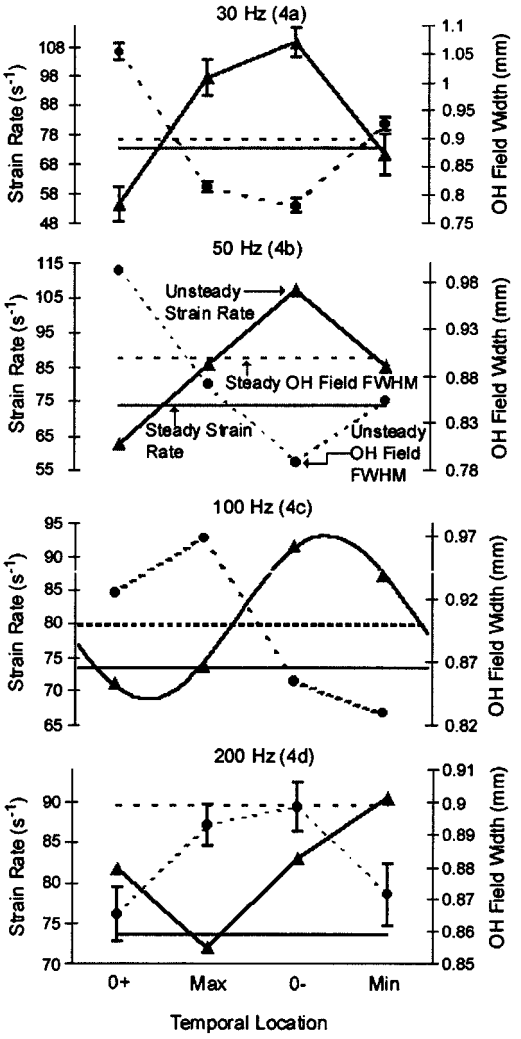

FIG. 4. Strain rate and FWHM of the OH field results for SSR $74 \cdot s^{-1}$ and all forcing frequencies. Error bars of one standard deviation have been included for the OH fields FWHM on the 30 Hz and 200 Hz forcing frequencies and for the strain rate at 30 Hz. Error bars for the measured strain rate are excluded on 4d as well as other plots for clarity, but the magnitudes are very similar to that shown in 4a. A sine wave curve is shown in 4c fitted to the strain rate.

and Min locations, the instantaneous strain rate decreases and the OH layer thickens. It was also found that when the instantaneous strain rate for the forced flames was above the steady strain rate, the OH field was thinner than the steady case. The converse of this was also found to be true. The strain rate and OH field behavior at a forcing frequency of 50 Hz mimicked the behavior found at 30 Hz, as seen in Fig. 4b. If the flame were responding steadily, increasing the strain rate would be accompanied by an increase in the convective velocities at the edge of the convective-diffusive zone of the flame. With this elevated supply of cool reactants, the flame would move closer to the stagnation plane, due to stoichiometry, and the flame would also cool and become thinner. Thinning of the flame with increasing strain rate has been found previously in experimental and numerical studies [10,11]. Thus, from Fig. 4a and b, the OH field, and hence the flame, is responding to the instantaneous strain rate in a quasi-steady manner, at forcing frequencies of 30 and 50 Hz. Note that cyclic behavior of the OH concentration has been found previously in a N_2 diluted methane/air flame [6].

As the forcing frequency was increased to 100 Hz, the strain rate was found to increase continuously between the temporal locations of 0+ and 0− and then decreased between the locations of 0− and Min, as seen in Fig. 4c. This is similar to the behavior found for lower-frequency oscillations. The OH field width was found to increase between the temporal location of 0+ and Max and then decreased continuously between the Max and Min locations. Thus, for the 100 Hz case, between the 0+ and Max locations, there is an increase in the instantaneous strain rate that is accompanied by an increase in the width of the OH layer. Also, between the 0− and Min locations, a decrease in the instantaneous strain rate is accompanied by a decreasing width of the OH layer. Similar behavior was also noted when the forcing frequency was increased to 200 Hz, which is shown in Fig. 4d. At 200 Hz, the strain rate decreased between 0+ and Max and then continuously increased between the Max and Min temporal locations. The OH field width increased between the locations of 0+ and 0− and then decreased between 0− and Min. Between the Max and 0− locations, there is an increasing strain rate and an increasing OH field width. Thus, the OH field does not respond quasi-steadily to the instantaneous strain rate at forcing frequencies above 100 Hz.

As illustrated in Fig. 4, the maximum strain rate occurs at the 0− temporal location for the three lower frequencies, but at the Min location for the 200 Hz case. Although a frequency-dependent phase-angle relationship between the strain rate and width of the OH field seems apparent, it cannot be directly deduced from Fig. 4. This is due to a frequency-dependent phase angle that exists between the speaker motion and the applied voltage [8]. Although only four temporal locations were measured for each flame condition, phase-angle relationships were still resolvable with this limited temporal sampling. Because the speakers are oscillating in a sinusoidal manner, previous studies have shown that parameters dependent upon their motion, such as the air exit velocity, respond similarly [6,8,12]. The

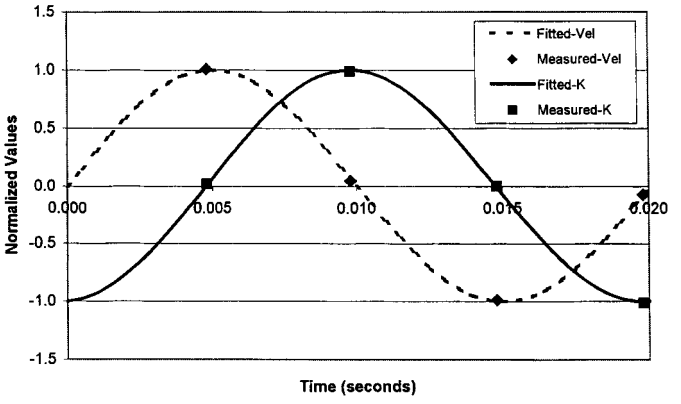

FIG. 5. Normalized velocity and strain rate data with their fitted curves for SSR 74 s^{-1} and 50 Hz.

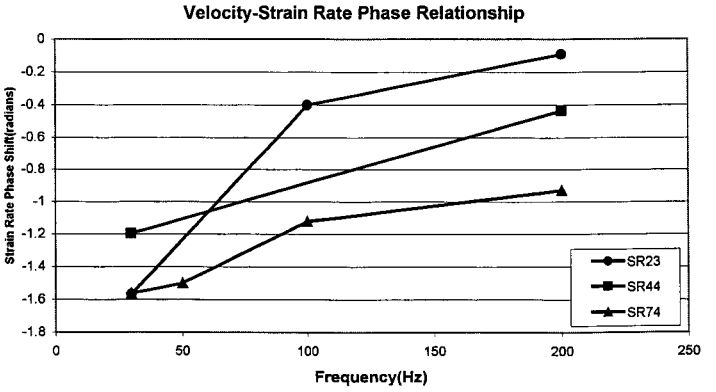

FIG. 6. Phase difference relationships between the air velocity and the strain rate as a function of frequency for initial steady strain rates of 23 s^{-1}, 44 s^{-1}, and 74 s^{-1}.

measured results of the velocity, strain rate, and the OH field were fitted to an offset sine function, as shown by equation 1, to determine phase-angle relationships.

$$V = V_0 + V_1 \cdot \sin(\omega \cdot t + V_2) \qquad (1)$$

Here, V_0 is an offset value, V_1 is half the peak-to-peak difference, V_2 is the phase difference, t is the temporal location in the oscillation, and ω is equal to $2\pi f$, where f is the forcing frequency. The parameters V_0, V_1, and V_2 were determined from the measured data.

Figure 5 shows a typical plot of the normalized measured velocity and strain rate with the corresponding fitted curves plotted versus time for a forcing frequency of 50 Hz. Subtracting V_0 and then dividing by V_1 normalizes the measured data and fitted curves. Good agreement was found between the measured data and the fitted sine functions. The velocity measurements reported in Fig. 5 correspond to the closest point to the flame that was not affected by heat release. This location was used because the relevant marker of the flowfield exists in the region where strain rate is measured instead of the nozzle exit [12]. This is a result of a phase difference between the air exit velocity and the velocities just prior to the preheat zone. As can be seen in Fig. 5, the strain rate is lagging the velocity. Under isothermal conditions or cyclic oscillations which have cycle times much longer than relevant transport times of the flame, the velocity and the strain rate will be in phase. Fig. 6 shows the phase-angle relationship between the velocity and strain rate as a function of frequency for SSRs of 23 s^{-1}, 44 s^{-1}, and 74 s^{-1}. For all strain rates, the phase difference between the strain rate and the velocity is decreasing as the forcing frequency is increased from 30 to 200 Hz. Egolfopoulos and Campbell [4] performed a detailed numerical study of the frequency response of counterflowing strained diffusion methane/oxygen/nitrogen flames. For a flame with a mean strain rate of 400 s^{-1}, they found the strain rate was in phase with the velocity for forcing frequencies below 10 Hz. Above forcing frequencies of 10 Hz, a phase difference was present between the strain rate and the air exit velocity, which reached a maximum and then began to decay back to zero as the forcing frequency continued to increased. The phase difference between the velocity and the strain rate was

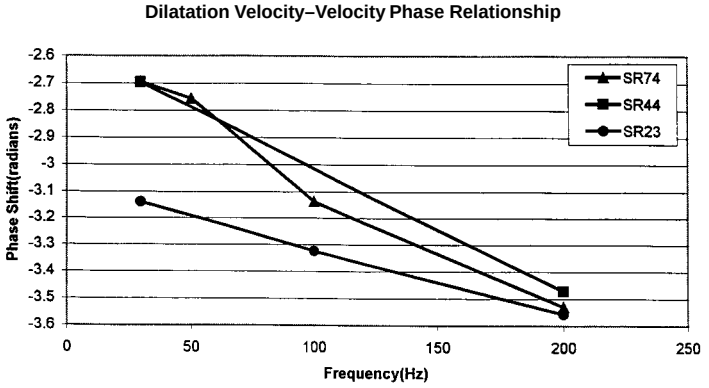

FIG. 7. Phase difference relationships between the dilatation velocity and the air velocity as a function of frequency for initial steady strain rates of 23 s^{-1}, 44 s^{-1}, and 74 s^{-1}.

found to be induced by a systematic increase in a lag between the velocity and thermal expansion, which follows the phase-shifted maximum cyclic temperature. The magnitudes of the oscillations in maximum temperature were also found to decrease as the forcing frequency increased. Sensitivity of strain rate to thermal expansion has been observed and investigated in previous studies [10,13,14]. Experimental results of the phase difference between velocity and strain rate presented in this study support the numerical results of Egolfopoulos and Campbell [4].

Figure 6 also illustrates that, generally, the phase difference between the velocity and strain rate is decreasing with decreasing initial steady strain rate. Increasing mean strain rates result in increased mean velocities at the edge of the convective-diffusive zone on the air side and thereby reduce the diffusive time necessary for the oxidizer to be transported to the reaction zone. Consequently, higher forcing frequencies will be necessary to induce a phase difference. An analogy has been presented between the attenuation of spatial gradients in viscosity for Stoke's second problem and the attenuation of spatial gradients of reactants with increasing forcing frequency [4]. With increasing strain rate, the frequency at which phase-shifted temperature (thermal expansion) effects decrease their influence on the strain rate will increase. Ultimately, this means an increasing strain rate should shift the location where the phase difference of the strain rate becomes non-zero, reaches a maximum, and decreases back to zero to higher forcing frequencies. The general trends shown in Fig. 6 support this description.

A flame temperature marker was derived to help confirm the phase-shifting behavior of the maximum temperature. Although no corrections for thermophoretic forces have been made to the velocities in the heat release zone, the difference between the maximum velocity in the reaction zone and the minimum velocity in the preheat zone, as shown in Fig. 3, was used as an indicator of the flame temperature. The increasing velocities in the reaction zone are a result of density changes resulting from heat release, so the general behavior of the changes in velocity should follow the temperature trend. This velocity difference will be referred to as the dilatation velocity. Fig. 7 shows the phase difference between the air velocity and the dilatation velocity as a function of frequency and initial steady strain rate. The magnitude of the phase difference was found to increase with increasing forcing frequency, which suggests there is a systematic increase in the phase difference between the velocity and the temperature. The time associated with the increasing phase difference is likely related to a diffusion time. As the forcing frequency is increased, the time rate of change of reactants delivered to the edge of the convective-diffusive zone increases; however, a finite amount of time is still necessary for the reactants to diffuse to the flame front. As the forcing frequency increases, this diffusion time becomes larger relative to the cycle time of the oscillation, which in turn shows up as an increasing phase difference. This diffusion-limited response has been observed in previous numerical studies [3,4].

Conclusions

The response of a propane/air counterflow diffusion flame subjected to an unsteady flowfield was investigated to increase fundamental understanding of turbulent flame behavior and to help qualify the quasi-steady assumption used in flamelet theory. The conclusions drawn from this investigation are as follows:

1. The width of the OH field appears to be responding quasi-steadily to the instantaneous strain rate for forcing frequencies of 30 Hz and 50 Hz; the calculated phase difference between the strain rate and width of the OH field are 183° and 185°, respectively. However, at forcing frequencies of 100 Hz and 200 Hz, the phase lag of the OH field thickness grew to 210° and 241°, respectively.

2. For the weakly forced flames presented in this report, the sinusoidal response of the velocity, strain rate, and width of the OH field correlated well with the speaker oscillations at the given frequency.
3. A phase difference was present between the velocity and the strain rate, which was found to decrease with increasing forcing frequency. This apparently results from the distortions imposed on the velocity field due to a phase-shifted thermal expansion.
4. The dilatation velocity was used as an indicator of flame temperature. The phase difference between the velocity and the dilatation velocity was found to increase with increasing forcing frequency. This increasing phase difference suggests the transport of reactants through the reactive-diffusive zone of the flame is the limiting step in the response of the flame sheet.

Acknowledgments

This work was supported by the Army Research Office, ARO grant number DAAH04-95-10230, under the technical monitoring of Dr. David Mann.

REFERENCES

1. Peters, N., *Prog. Energy Combust. Sci.* 10:319–339 (1984).
2. Bray, K. N. C., and Peters, N., *Turbulent Reacting Flows,* Academic Press, Orlando, FL, 1994, p. 63.
3. Im, H. G., Law, C. K., Kim, J. S., and Williams, F. A., *Combust. Flame* 100:21–30 (1995).
4. Egolfopoulos, F. N., and Campbell, C. S., *J. Fluid Mech.* 318:1–29 (1996).
5. Darabiha, N., *Combust. Sci. Technol.* 86:163–181 (1992).
6. Brown, T. M., Pitz, R. W., and Sung, C. J., *Proc. Combust. Inst.* 27:703–710 (1998).
7. Puri, I. K., and Seshadri, K., *Combust. Flame* 65:137–150 (1986).
8. DeCroix, M. E., and Roberts, W. L., *Combust. Sci. Technol.* 146:57–84 (1999).
9. Sung, C. J., Kistler, M., Nishioka, M., and Law, C. K., *Combust. Flame* 105:189–201 (1996).
10. Sung, C. J., Liu, J. B., and Law, C. K., *Combust. Flame* 102:481–492 (1995).
11. Pellett, G. L., Isaac, K. M., Humphreys Jr., W. M., Gartrell, L. R., Roberts, W. L., Dancey, C. L., and Northam, G. B., *Combust. Flame* 112:575–592 (1998).
12. Kistler, J. S., Sung, C. J., Dreutz, T. G., Law, C. K., and Nishioka, M., *Proc. Combust. Inst.* 26:113–120 (1996).
13. Kim, J. S., Libby, P. A., and Williams, F. A., *Combust. Sci. Technol.* 87:1–25 (1992).
14. Zhoa, J., Isaac, K. M., and Pellett, G. L., *J. Propul. Power* 12:3 (1996).

COMMENTS

Sébastien Candel, Ecole Centrale Paris, France. One characteristic time of a strained diffusion flame is just the inverse of the strain rate. This could be used to define a dimensionless frequency and this might allow collapsing the data gathered in these experiments.

Author's Reply. Following the work of Egolfopoulos and Campbell [4], a dimensionless Stokes parameter may be defined as (pf/k) 1/2, where f is the forcing frequency and k is the steady strain rate. If the change in thickness of the OH zone through the oscillation, normalized by the steady thickness, is plotted against the log of this Stokes' parameter, all the data from the four forcing frequencies (30, 50, 100, and 200 Hz) and three different initial strain rates (23, 44, and 74 s^{-1}) collapse very well onto a single line with a fairly steep negative slope. The Stokes' parameter ranges from 1 to 6 in these experiments; Ref. 4 shows a negative slope when the normalized maximum temperature is plotted over this range as well.

•

Jay Jeffries, Stanford University, USA. Could you quantify the uncertainty on temperature and spatial resolution? It appears you have drawn conclusions from temperature variation of 15 K and spatial (OH FWHM) variations of tens of micrometers.

Author's Reply. Figure 4 has been updated with the correct y-axis scaling; the figure shown during the talk and to which you are referring was off by a factor of 3.5. Thus, the actual maximum delta in OH field width throughout the oscillations range from 280 mm at 30 Hz to 31 mm at 200 Hz. While these differences are small, from 3% to 30% of the steady width (880 mm), they are real and very repeatable. The axial OH profile was averaged about the centerline in the radial direction over 3 mm (spatial resolution of 50 mm/pixel), and 20 OH PLIF images at each location within the oscillation were averaged to get the final OH field width. The standard deviation of the mean among these 20 images was typically less than 0.25% and always less then 1%. Thus, while our smallest delta in field width is 0.6 pixels wide, due to the radial averaging, we believe this is a real result. The standard deviation of the mean in temperature is very similar. So, while the absolute temperatures are no better than to within say 100 K, the relative temperatures throughout the oscillation are much better. Further details regarding the thermometry data is forthcoming.